K. M. Pranesh Rao[1] and Narayan Prabhu[2]

# Estimation of Spatially Dependent Heat Flux Transients during Quenching of Inconel Probe in Molten Salt Bath

## Reference

[1] Department of Metallurgical and Materials Engineering, National Institute of Technology Karnataka, Surathkal, Mangalore-575025, India

[2] Department of Metallurgical and Materials Engineering, National Institute of Technology Karnataka, Surathkal, Mangalore-575025, India (Corresponding author), e-mail: prabhukn_2002@yahoo.co.in

## ABSTRACT

Several industrial heat treatment processes, such as martempering and austempering, require a quench bath to be maintained at a temperature ranging between 150°C–600°C. Molten salts, molten alkali, and hot oils are the preferred quenchants for these processes. Molten salts and molten alkali are preferred over hot oil because they possess properties like wide operating temperature range, excellent thermal stability, and tolerance for contaminants. In the present work, the performance of a molten potassium nitrate ($KNO_3$) quench bath was analyzed with an Inconel probe that measured 60 mm in height and 12.5 mm in diameter. The probe was heated to 850°C and subsequently quenched in a bath maintained at 450°C. Cooling curves at different locations of the probe were recorded using the K-type thermocouples inserted into the probe. Spatially dependent transient heat flux at the metal/quenchant interface was estimated using inverse heat conduction technique. The existence of two stages of quenching—boiling stage and convection stage—was confirmed by analyzing the heat flux. The heat transfer coefficient was calculated based on heat flux obtained by the inverse method. The nonuniformity in heat transfer along the length of the probe was quantified by calculating the range of surface temperatures at each instance. The hardness distribution in an AISI 4140 steel was predicted using the temperature distribution in the Inconel probe and obtained using inverse method. Uneven distribution of hardness predicted in the probe was attributed to the nonuniform cooling of the probe during quenching.

## Nomenclature

$$
\begin{aligned}
r &= \text{Radial direction in polar coordinate system, mm} \\
z &= \text{Axial direction in polar coordinate system, mm} \\
q &= \text{Spatially dependent transient heat flux, kW/m}^2 \\
p_1, p_2, p_3, &= \text{Parameters in cubic equation for estimation of } q \\
\text{and } p_4 & \\
P &= \text{Vector representation of parameters } p_1, p_2, p_3, \text{ and } p_4 \\
k &= \text{Thermal conductivity in W/mk} \\
\rho &= \text{Density kg/m}^3 \\
C_p &= \text{Specific heat in J/kgK} \\
t &= \text{Time in s} \\
Y &= \text{Measured temperature vector} \\
T &= \text{Calculated temperature vector} \\
S &= \text{Objective function} \\
\beta &= \text{Search step size} \\
\gamma &= \text{Conjugation coefficient} \\
d &= \text{Direction of descent vector} \\
J &= \text{Jacobian Matrix} \\
\varepsilon &= \text{Convergence criterion} \\
T_{Cmeas} &= \text{Temperature measured at the geometric center of the probe, °C} \\
T_{Ccalc} &= \text{Temperature calculated at the geometric center of the probe, °C} \\
\% \text{ Error} &= \text{Percentage of error between measured and calculated values of temperature} \\
q_{Avg} &= \text{Spatially dependent heat flux averaged over space, kW/m}^2 \\
T_{Avg} &= \text{Mean surface temperature, K} \\
dq/dt &= \text{Derivative of } q_{Avg} \text{ with respect to time} \\
T_b &= \text{Quench bath temperature} \\
h_{Inverse} &= \text{Heat transfer coefficient calculated using inverse method, W/m}^2\text{K} \\
\bar{h}_{Inverse} &= \text{Average heat transfer coefficient during quenching, W/m}^2\text{K} \\
q_{max} &= \text{Peak heat flux, kW/m}^2 \\
q_{Range} &= \text{Range of surface heat flux} \\
T_{Range} &= \text{Range of surface temperature} \\
E &= \text{Energy extracted per unit area, kJ/m}^2 \\
t_{85} &= \text{Time of cooling from 800°C to 500°C in s}
\end{aligned}
$$

## Introduction

Austempering and martempering heat treatment processes require quench media that can sustain a temperature range of 150°C–600°C without degrading. The quenchant maintained at a temperature well above room temperature is expected to rapidly cool the austenized metal part near quench bath temperature. Rapid cooling of the austenized part avoids undesired diffusion-based transformations in the steel. Hot oils (marquench oils), molten mixtures of alkali nitrate/nitrite salts, alkali chloride salts, alkali hydroxides and carbonates, and some metals/alloys are used as high-temperature quench media.

Molten salt baths have been used in the heat treatment industry as quench media for more than fifty years. Molten salts possess properties such as wide operating temperature ranges, excellent thermal stability, and tolerance for contaminants. These properties make salt quenching systems almost maintenance-free and thus can provide satisfactory performance for many years simply by replenishing dragged out salt quench media.

Molten mixtures of sodium and potassium nitrate/nitrites, also known as saltpeter salts, are the most commonly used high-temperature quench media. The melting points of these mixtures depend on their compositions. Mixtures of salts that have melting points ranging between 440°C and 150°C can be obtained. Dubal [1] suggested choosing a salt mixture so that the operating temperature is at least 50°C greater than its melting temperature.

Potassium nitrate ($KNO_3$) salt has a melting pint of 334°C and is widely used as a quench medium to heat treat steels. In the present work, the cooling performance of the $KNO_3$ quench medium maintained at a temperature of 450°C was evaluated.

## Experiment

An Inconel probe instrumented with thermocouples (**Fig. 1b**) was used to characterize the cooling performance of the quench medium. The probe was a cylinder measuring 60-mm tall and 12.5-mm wide, with a 5-mm-long M16 thread at top. K-type Inconel sheathed thermocouples with 1-mm diameters were inserted into 1-mm diameter Electrical discharge  machining (EDM)-drilled holes in the probe through a stainless steel tube. The probe had five holes, one at the center with a depth of 30 mm and four that were 2 mm from the surface of the probe, reaching to depths of 7.5 mm, 22.5 mm, 37.5 mm, and 52.5 mm (the listed depths are exclusive of the 5-mm thread at the top of the probe). The

**FIG. 1**  (a) Setup for quenching experiments. (b) Schematic of quench probe.



(a)                                                                 (b)
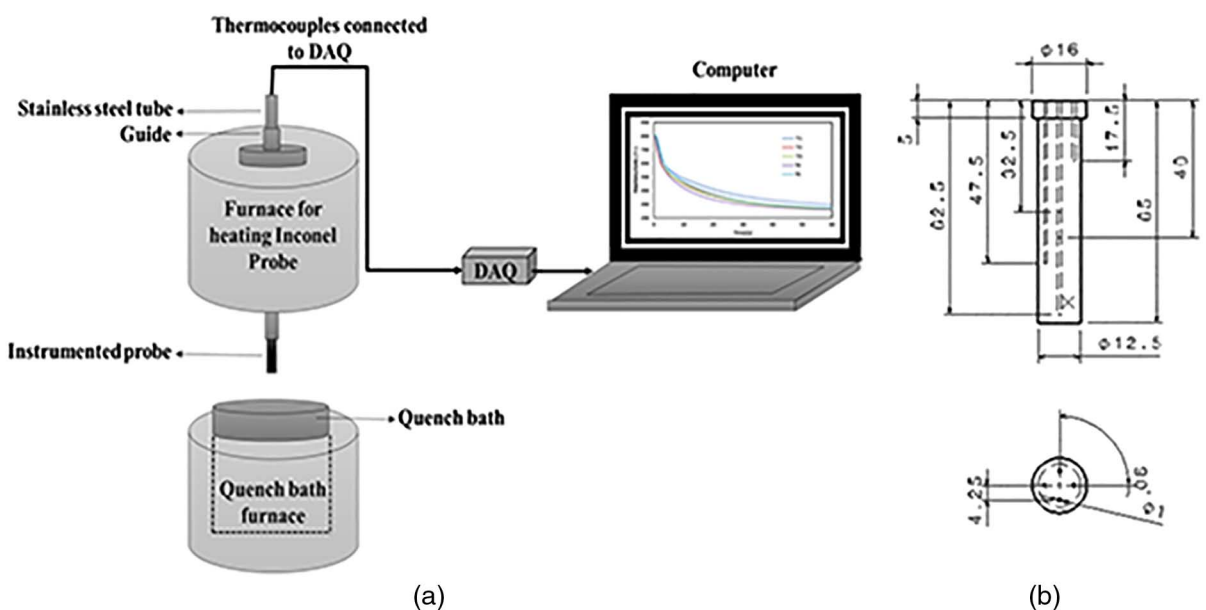
M16 thread of the probe was fastened to the stainless steel tube, and the instrumented probe was then heated in a vertical tubular furnace to a temperature of 850°C. Subsequently, the stainless steel tube was lowered through a guide and the probe was quenched in the quench bath. A quench bath furnace was used to melt the $KNO_3$ and maintain the molten quench bath at 450°C. Cooling curves were recorded in the computer through a NI-9213 data logger. The thermocouples were connected to the data logger through compensating cables. Temperature data were acquired at a time interval of 0.1 s.

### INVERSE HEAT TRANSFER TECHNIQUE

Time temperature data recorded by thermocouples located near the surface of the probe during quenching were used to estimate spatially dependent transient heat flux at the metal/quenchant interface. The locations of these thermocouples are designated as $TC_1$, $TC_2$, $TC_3$, and $TC_4$ in **Fig. 4**. Temperature data recorded at the geometric center of the probe were used to validate the estimated heat flux.

As shown in **Fig. 2**, the probe was considered axisymmetric, and heat transfer from top and bottom surfaces of the probe were assumed to be 0. Heat transfer at the metal/quenchant interface was modeled as a cubic function of distance $z$ measured from the bottom of the probe. The parameters $p_1$, $p_2$, $p_3$, and $p_4$ were estimated for each time step using inverse heat transfer technique. The conjugate gradient method suggested by Őzisik and Orlande [2] was used to estimate these parameters. The inverse heat transfer technique requires the heat conduction equation (Eq 1) to be solved. Finite element method (FEM) was used to solve the heat conduction equation. A 60-by-6.25 mm axisymmetric rectangular model of the probe was discretized into 6,000 square elements that

**FIG. 2**

Axisymmetric model of probe used to estimate spatially dependent transient heat flux at the metal/quenchant interface.
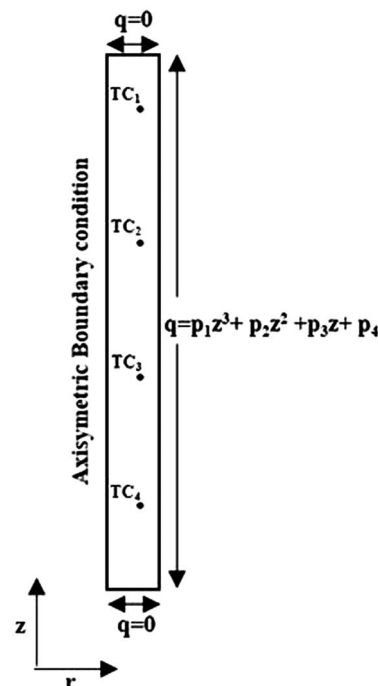
## TABLE 1
Temperature dependent thermal properties of Inconel 600 alloy [3].

| T (°C) | 200 | 250 | 300 | 350 | 400 | 450 | 500 | 600 | 700 | 800 | 900 |
|---|---|---|---|---|---|---|---|---|---|---|---|
| k (W/mK) | 16 | 16.9 | 17.8 | 18.7 | 19.7 | 20.7 | 21.7 | – | 25.9 | – | 30.1 |
| Cp (J/kgK) | 491 | – | 509 | – | 522 | – | 533 | 591 | 597 | 597 | 611 |
| ρ (kg/m3) | 8,340 | – | 8,300 | – | 8,270 | – | 8,230 | 8,190 | 8,150 | 8,100 | 8,060 |

measured 0.25 by 0.25 mm. Temperature-dependent thermal properties of Inconel used to solve FEM are stated in Table 1.

$$\frac{\partial}{\partial r}\left(kr\frac{\partial T}{\partial r}\right) + \frac{\partial}{\partial z}\left(k\frac{\partial T}{\partial z}\right) = \rho C_p \frac{\partial T}{\partial t} \tag{1}$$

The inverse problem was solved by estimating parameters $p_{1,ts}$, $p_{2,ts}$, $p_{3,ts}$, and $p_{4,ts}$ for which the objective function $S_{ts}$ is minimized at each time step $ts$,

Parameters can be represented in vector form as $P$ in the following:

$$P_{ts} = [p_{1,ts}\ p_{2,ts}\ p_{3,ts}\ p_{4,ts}] \tag{2}$$

$$q(P_{ts}, z) = p_{1,ts}z^3 + p_{2,ts}z^2 + p_{3,ts}z + p_{4,ts} \tag{3}$$

where $z$ varies between 0 and 60 mm.

$$S_{ts} = \sum_{i=1}^{n}\sum_{j=1}^{m}\left(Y_{i,ts+j-1} - T(P_{ts})_{i,ts+j-1}\right)^2 \tag{4}$$

where $Y_{i,ts+j-1}$ is the temperature measured at $i^{th}$ location and $ts+j-1^{th}$ time step. Since the temperature was measured at four locations, $n = 4$, $T(P_{ts})$ was calculated using FEM by assuming that heat flux remains constant for the next $m$ time steps. In the present work, the number of future times steps ($m$) was assumed to be four.

In vector form, Eq 5 can be written as the following:

$$S_{ts} = [Y_{ts} - T(P^k{}_{ts})]^T[Y_{ts} - T(P^k{}_{ts})] \tag{5}$$

where $Y$ and $T$ are vectors of measured and calculated vectors written as follows:

$$Y_{ts} = [Y_{1,ts}Y_{1,ts+2}Y_{1,ts+2}\cdots\cdots\cdots Y_{i,ts+j-1}\cdots\cdots\cdots\cdots\cdots Y_{n,ts+m}]^T \tag{6}$$

$$T(P^k{}_{ts}) = [T_{1,ts}T_{1,ts+2}T_{1,ts+2}\cdots\cdots\cdots\cdots T_{i,ts+j-1}\cdots\cdots\cdots\cdots\cdots T_{n,ts+m}]^T \tag{7}$$

The solution for the inverse problem involves an iterative algorithm that is presented in Fig. 3.

$\beta^k_{ts}, \gamma^k_{ts}$, and $d^k_{ts}$ are search step size, conjugation coefficient, and the direction of descent, respectively. $J^k_{ts}$ is sensitivity matrix of dimension 16 by 4, which was defined as the following:

$$J^k_{ts} = \left[\frac{\partial T(P^k_{ts})}{\partial p_{1,ts}}\ \frac{\partial T(P^k_{ts})}{\partial p_{2,ts}}\ \frac{\partial T(P^k_{ts})}{\partial p_{3,ts}}\ \frac{\partial T(P^k_{ts})}{\partial p_{4,ts}}\right] \tag{8}$$

**FIG. 3**

Inverse solution algorithm.

1) $k=0$, $P_{ts}^0 = [-1000\ -1000\ -1000\ -1000]$ where k is the iteration step number k=0,1,2……

2) $\nabla S_{ts}^k = -2(J_{ts}^k)^T[Y_{ts} - T(P_{ts}^k)]$

3) $\gamma^k = \sum \dfrac{(\nabla S_{ts}^k)^2}{(\nabla S_{ts}^{k-1})^2}$ If k=0, $\gamma_{ts}^k = 0$

4) $d_{ts}^k = \nabla S_{ts}^k + \gamma_{ts}^k d_{ts}^{k-1}$

5) $\beta_{ts}^k = \dfrac{(J_{ts}^k d_{ts}^k)^T(T(P_{ts}^k)-Y_{ts})}{(J_{ts}^k d_{ts}^k)^T(J_{ts}^k d_{ts}^k)}$

6) $P_{ts}^{k+1} = P_{ts}^k - \beta_{ts}^k d_{ts}^k$

7) $\varepsilon = \dfrac{\sqrt{\sum\left(q(P_{ts}^{k+1},z)-q(P_{ts}^k,z)\right)^2}}{\sqrt{\sum q(P_{ts}^{k+1},z)^2}}$

where z=0, 0.25, 0.5, ……60mm

8) If $\varepsilon < 5 \times 10^{-3}$ stop iteration and proceed to next time step, else **k=k+1** and go to step 2

The partial derivatives in $J_{ts}^k$ is calculated using the following Eq 9:

$$\frac{\partial T(p_{ts}^k)}{\partial p_{1,ts}} = \frac{T([p_{1,ts}^k + \delta p_{1,ts},\ p_{2,ts}^k,\ p_{3,ts}^k,\ p_{4,ts}^k]) - T([p_{1,ts}^k,\ p_{2,ts}^k,\ p_{3,ts}^k,\ p_{4,ts}^k])}{\delta P_{1,ts}} \quad (9)$$

where, $\delta p_{1,ts} = 10^{-4} \times p_{1,ts}$

$T([p_{1,ts} + \delta p_{1,ts},\ p_{2,ts},\ p_{3,ts},\ p_{4,ts}])$ and $T([p_{1,ts}^k,\ p_{2,ts}^k,\ p_{3,ts}^k,\ p_{4,ts}^k])$ in Eq 9 were evaluated by solving the heat conduction equation using FEM. Similarly, the partial derivative of the temperature vector with respect to the other three parameters (i.e., $p_{2,ts}$, $p_{3,ts}$, and $p_{4,ts}$) were evaluated. The converged values of $p_{1,ts}$, $p_{2,ts}$, $p_{3,ts}$, and $p_{4,ts}$ at each time step were used to calculate spatially dependent heat flux at that time step using Eq 3.

## Results and Discussion

In **Fig. 4**, $Y_1$, $Y_2$, $Y_3$, and $Y_4$ are the temperature data measured at locations $TC_1$, $TC_2$, $TC_3$, and $TC_4$ (shown in **Fig. 2**), respectively. The measured temperature data ($Y_1$, $Y_2$, $Y_3$, and $Y_4$) were used to estimate the spatially dependent transient heat flux. **Fig. 5** shows spatially dependent heat flux transients calculated for the first ten seconds of quenching. The rate of extraction of heat at the metal/quenchant interface rapidly increased to a maximum value of 1.5 s at all locations. The heat flux slowly decreased thereafter and approached 0 W as the temperature of the probe nearly equalled the bath temperature. The magnitude of heat flux was observed to vary considerably with space ($z$).

The temperature data acquired at the geometric center of the probe were not used to calculate the heat flux using inverse method. Equation **10** was used to calculate *% Error* between measured temperature ($T_C meas$) and calculated temperature ($T_C calc$) at the geometric center of the probe. During quenching, *% Error* was observed to be negligibly small, its maximum value being 0.8% as evident from **Fig. 6**. The low value of *% Error* proves the

**FIG. 4**

Temperature data measured by the thermocouples placed near the surface of the probe.
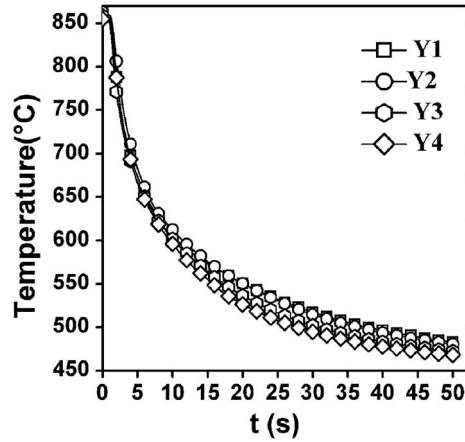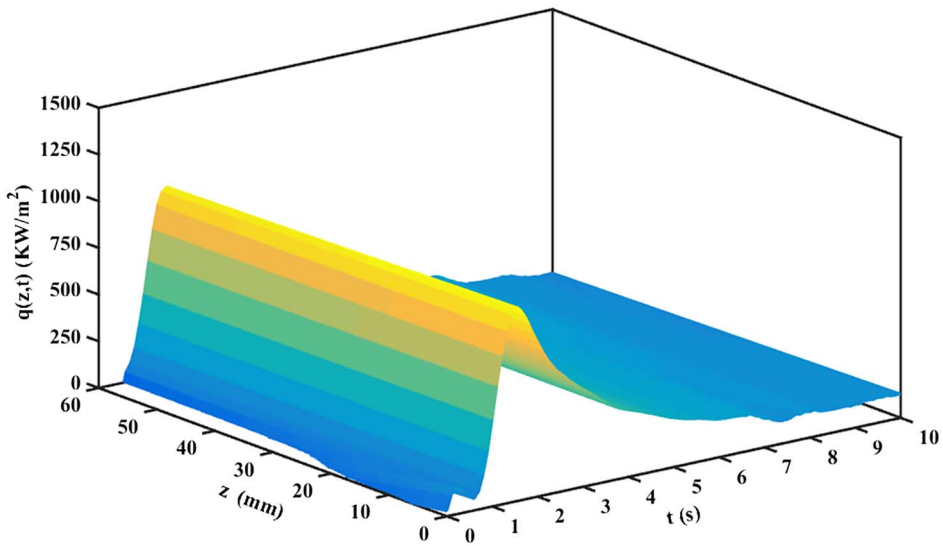


**FIG. 5** Heat flux as a function of time and space calculated using inverse method.



accuracy of the estimated spatially dependent transient heat flux calculated using inverse method, as follows:

$$\% \ Error(t) = \frac{(T_{C_{meas}}(t) - T_{C_{calc}}(t)) \times 100}{(T_{C_{meas}}(t))} \tag{10}$$

**AVERAGE HEAT FLUX**

Spatially dependent transient heat flux and surface temperatures estimated using the inverse heat conduction method were averaged over the length of the probe. Average surface temperature ($T_{Avg}$) and average surface heat flux ($q_{Avg}$) were calculated at each time step. Furthermore, the first derivative of $q_{Avg}$ with respect to time ($dq/dt$) was calculated.

**FIG. 6**

Transient variation of *% Error* between calculated and measured values of temperature at the geometric center of the probe.
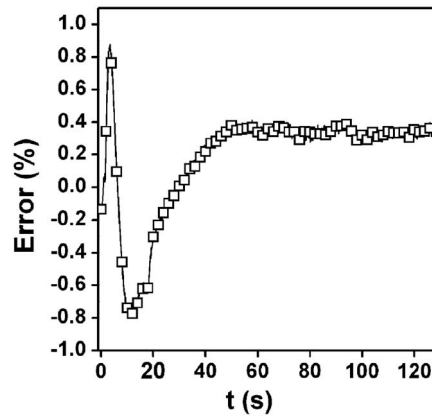


Fig. 7 shows the variation of $q_{Avg}$ and *dq/dt* with $T_{Avg}$. The vapor blanket stage observed in most of the conventional quench media (water, brine, mineral oil) [4] was absent during quenching in the KNO$_3$ quench. While quenching the probe that was heated to 850°C in the molten KNO$_3$ bath, heat transfer occurred initially when the boiling quenchant came in contact with the probe surface. This stage is generally referred to as boiling or nucleate boiling stage. $q_{Avg}$ rapidly increased to Point A and then decreased slowly to Point B. Point B is the point where the transition of the heat transfer mechanism from boiling stage to convection stage occurs. During the convection stage, the second stage of cooling, the heat transfer at the metal/quenchant interface occurred due to natural convection. Heat flux was observed to be very high during boiling stage and $q_{Avg}$ reached the maximum value (at Point A) of 1,020 kW/m$^2$, and the corresponding value of $T_{Avg}$ was 745°C. The energy extracted during the boiling stage was 95 % of total heat removed

**FIG. 7**

Variation of *qAvg* and *dq/dt* with $T_{Avg}$.
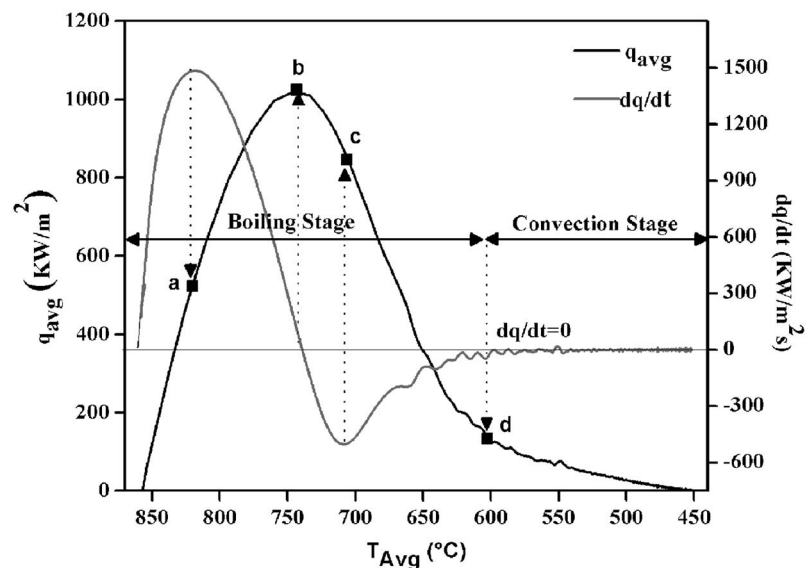
during quenching. The magnitude of heat flux during the convection stage was observed to be very low and approached 0 as $T_{Avg}$ approached the quench bath temperature of 450° C. At transition Point B, $T_{Avg}$ was nearly equal to 604°C and $q_{Avg}$ reached a value of 149 kW/m².

## HEAT TRANSFER COEFFICIENT

The heat transfer coefficient was calculated using average heat flux $q_{Avg}$ and surface temperature $T_{Avg}$ using Eq 11. **Fig. 8** shows the variation of the transient variation heat transfer coefficient calculated using inverse method with $T_{Avg}$. The value of maximum heat transfer coefficient was 3,545 W/m² K. The average heat transfer coefficient over the entire range of temperatures during quenching was calculated as $\bar{h}_{Inverse} = 1{,}658$ W/m²K.

$$h_{Inverse} = \frac{q_{Avg}}{T_{Avg} - T_b} \tag{11}$$

## NONUNIFORM COOLING DURING QUENCHING

Nonuniform cooling during quenching would invariably result in microstructure variation, distortion, or residual stress in the quenched part [5]. **Fig. 9** shows the variation of the maximum value of heat flux ($q_{max}$) and energy removed ($E$) with distance from the bottom of the probe ($z$). The value of both parameters $q_{max}$ and $E$ was observed to be higher at the bottom portion and lower at the top portion of the probe. Thus, there exists a significant difference in heat transfer rates along the surface of the probe; more energy was removed in the bottom part of the probe compared to the top part of the probe.

The variation of heat flux along the surface of the probe results in the variation of surface temperature along the length of the probe. Stochastic parameter "RANGE," defined as the difference between maximum and minimum, was used to quantify the cooling nonuniformity. The range of surface temperature ($T_{Range}$) and range of heat flux ($q_{Range}$) were calculated at each time step. **Fig. 10** shows the variation of $T_{Range}$ and $q_{Range}$ with

**FIG. 8**

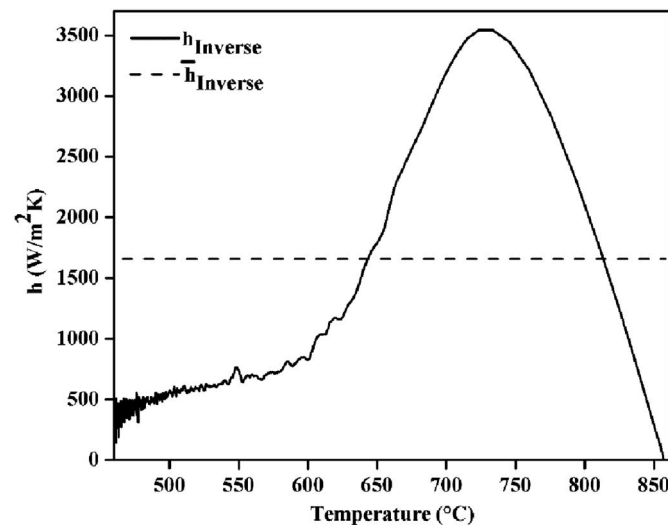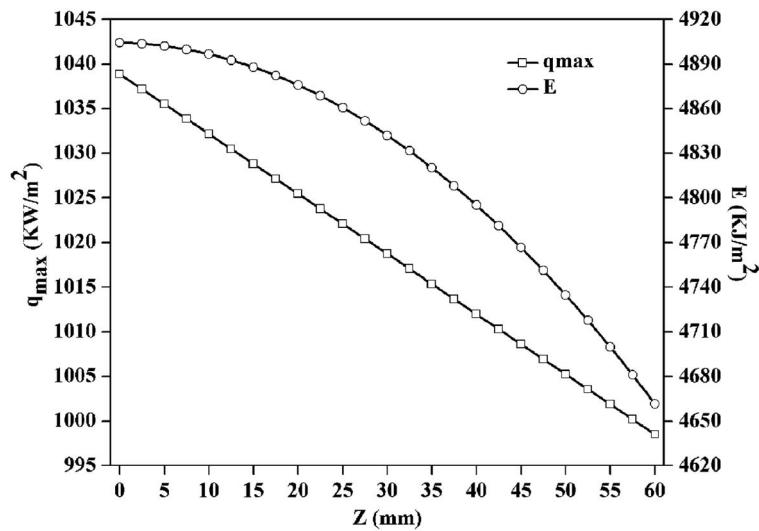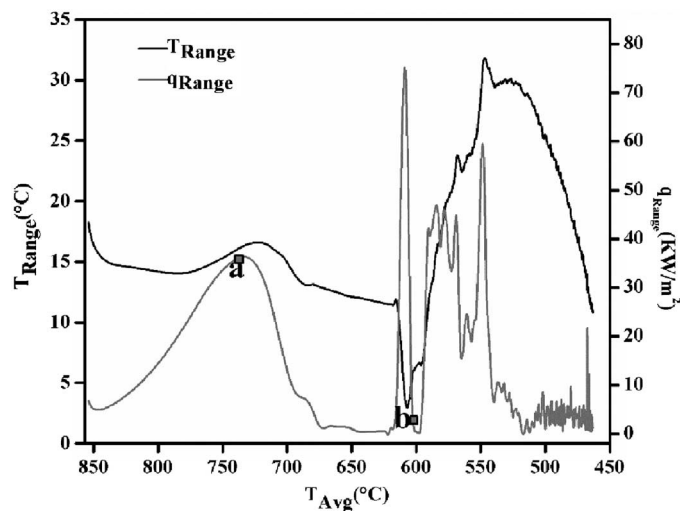Variation of heat transfer coefficient with $T_{Avg}$.

**FIG. 9**

Variation of maximum heat flux and energy removed with distance.



**FIG. 10**

Variation of range of surface temperature and heat flux with $T_{Avg}$.



$T_{Avg}$. The points A and B are the points that correspond to the maximum value of $q_{Avg}$ during the boiling stage and the transition from boiling to convection stage, respectively.

The variation in heat flux along the surface of the probe increased with the increase in the magnitude of heat flux during the boiling stage, and reached local maximum when $q_{Avg}$ approached maximum value at Point A. The variation in heat flux then decreased and reached minimum near Point B. The variation in surface temperature remained nearly constant at around 15°C during the boiling stage, barring a small increase near Point A. The observed variation in the heat flux became unstable and varied immensely when the boiling stage ceased and the convection stage resumed near Point B. Subsequently, during the convection stage, $q_{Range}$ decreased to a minimum value, and a very low heat

transfer rate was observed during this stage. The variation in surface temperature reached a minimum near Point B, suggesting high uniformity in surface temperature at the start of the convection stage. The nonuniformity in surface temperature increased to a maximum value during the convection stage, and after reaching maximum, $T_{Range}$ decreased. It was observed that nonuniformity in surface temperature was higher in the convection stage than the boiling stage. Low nonuniformity in surface temperature in the martensitic transformation range abated distortion and residual stress in the quenched part.

Apart from residual stress and distortion, nonuniform cooling along the surface of the probe resulted in nonuniform hardness distribution in the probe. Fig. 11 shows the simulated distribution of hardness in an AISI 4140 alloy probe with the same dimensions as that of the Inconel probe used for the experiment. Continuous cooling transformation (CCT) curves were simulated for AISI 4140 steel in JMatPro software. JMatPro software was used to predict hardness with known value of parameter $t_{85}$, i.e., the time required to cool from 800°C to 500°C. The parameter $t_{85}$ was calculated using temperature distribution in the probe. Furthermore, the calculated values of $t_{85}$ were used to model hardness distribution in the probe.

Fig. 11 clearly establishes the effect of spatially dependent heat flux transient on hardness distribution in an AISI 4140 probe. Hardness varied from 50.8 HRC to 55.25 HRC. The hardness was observed to be high in the lower part of the probe and low in the upper

**FIG. 11**

Simulated hardness distribution in the axisymmetric AISI 4140 probe.
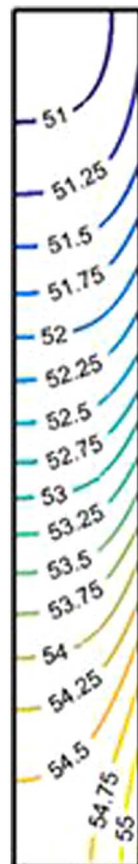
part of the probe. The predicted uneven hardness distribution was attributed to the nonuniform cooling of the probe during quenching.

## Conclusions

Based on the spatially dependent heat flux transients obtained for quenching a hot Inconel probe in molten $KNO_3$ bath maintained at 450°C, the following conclusions were drawn:

- The vapour blanket stage was absent and heat transfer to the quench medium occurred during boiling and convective stages.
- The maximum heat flux during the boiling stage occurred 1.5 s after the start of quenching. The maximum average heat flux of 1,020 $kW/m^2$ occurred when the average surface temperature reached 745°C. The convection stage started when the average surface temperature dropped to 604°C, and the corresponding heat flux was found to be 149 $kW/m^2$.
- The value of average and maximum heat transfer coefficients during quenching were 1,658 $W/m^2K$ and 3,545 $W/m^2K$, respectively.
- The heat energy extracted from the bottom of the probe was considerably higher compared to that which was extracted from the upper part of the probe, indicating nonuniform cooling of the probe.
- The nonuniformity in surface temperature, quantified by $T_{Range}$, was nearly constant at about 15°C during the boiling stage.
- The surface temperature was nearly uniform at the beginning of the convection stage.
- During convection stage, the nonuniformity in the surface temperature increased to the maximum value and then decreased. The nonuniformity in the surface temperature was higher than that during the boiling stage.
- The hardness values predicted in an AISI 4140 steel probe of the same dimensions as the Inconel probe were lower at the bottom part of the probe and higher in the top part of the probe. Nonuniform cooling of the probe resulted in uneven distribution of predicted hardness in the probe.

## References

[1] Dubal, G. P., "Salt Bath Quenching," *Adv. Mater. Proc.*, Vol. 156, No. 6, 1999, pp. 23–28.

[2] Özisik, M. N. and Orlande, H. R. B., *Inverse Heat Transfer: Fundamentals and Applications*, CRC Press, Boca Raton, FL, 2000, p. 352.

[3] Ramesh, G. and Prabhu, K. N., "Spatial Dependence of Heat Flux Transients and Wetting Behaviour During Immersion Quenching of Inconel 600 Probe in Brine and Polymer Media," *J. Metall. Mater. Trans. B.*, Vol. 45, No. 4, 2014, pp. 1355–1369, https://doi.org/10.1007/s11663-014-0038-7

[4] Liscic, B., Tensi, H. M., Canale, L. C. F., and Totten, G. E., Eds., *Quenching Theory and Technology*, 2nd ed., CRC Press, Boca Raton, FL, 2010, p. 725.

[5] Totten, G. E., Bates, C. E., and Clinton, N. A., *Handbook of Quenchants and Quenching Theory*, ASM International, Materials Park, OH, 1993, p. 507.